



# Oxidative dehydrogenation of ethane with oxygen catalyzed by K–Y zeolite supported first-row transition metals

Xufeng Lin, Kenneth R. Poepelmeier, Eric Weitz\*

Department of Chemistry and Institute for Catalysis in Energy Processes, Northwestern University, 2145 Sheridan Road, Evanston, IL 60208, USA

## ARTICLE INFO

### Article history:

Received 21 October 2009

Received in revised form 19 March 2010

Accepted 24 March 2010

Available online 31 March 2010

### Keywords:

Oxidative dehydrogenation

Ethane

First-row transition metals

Y zeolite

## ABSTRACT

Fe, Co, Ni, and Cu oxide loaded K–Y zeolites were synthesized using a two-step method, in which transition metals in the zeolite framework reacted with the anions in solution to form an insoluble salt which, when calcined, is expected to form an oxide that is anchored to the inner and/or outer zeolite surface(s). The catalytic properties of these zeolites, for the oxidative dehydrogenation of ethane (ODHE) to ethylene were then investigated. An ethylene selectivity of close to 80%, at an ethane conversion of >20% was achieved on a nickel oxide loaded K–Y catalyst. This is a higher ethylene selectivity, at higher ethane conversion, than was achieved using a previously reported Ni/KY catalyst. The effects of both reaction temperature and the  $O_2/C_2H_6$  ratio on the catalytic performance were examined. The apparent energy of activation for the ODHE reaction on the nickel oxide loaded K–Y catalyst was  $51.5 \pm 0.7$  kJ/mol. The  $C_2H_4$  selectivity at zero conversion ( $S_0$ ) on nickel oxide loaded K–Y was estimated for various  $O_2/C_2H_6$  ratios at a number of temperatures. The implications for the reaction mechanism of the  $S_0$  values, with regard to the relative values of critical rate constants are discussed.

© 2010 Elsevier B.V. All rights reserved.

## 1. Introduction

Over 100 million metric tons of ethylene are produced annually [1], with steam cracking of longer chain hydrocarbons being the primary method for ethylene production [2]. Oxidative dehydrogenation (ODH) of ethane (ODHE) is potentially a lower energy and less capital intensive method for the production of ethylene. Petroleum is currently the main feedstock for the steam cracking. Since petroleum is expected to be exhausted many years before natural gas, a source of short chain alkanes, it is desirable to develop chemical processes that employ small alkanes to yield more chemically useful olefins.

Although a large body of ODHE research has been reported, no ODHE process is currently a clear candidate to replace steam cracking [3]. This is primarily because catalysts are not available that give high conversions of alkanes along with high selectivity for alkenes. In the literature ODH catalysts can be divided into three categories [4]: catalysts based on (i) reducible metal oxides, (ii) noble metal-based catalysts, primarily Pt-based catalysts, and (iii) catalysts that generate radicals to initiate homogenous reactions in the gas phase (these typically contain alkali earth oxides and oxides of rear earth metals). For the first type of catalysts, vanadium and molybdenum oxide-based catalysts have been studied most extensively [3,5–8]. In contrast, there has been less work with the

first-row group VIII metals for ODH catalysis [9–11]. However, since these metals are plentiful and relatively inexpensive they would be highly desirable as catalysts. Additionally, reports on ODHE reactions using zeolite supports, especially microporous zeolites, are relatively sparse [12,13]. In previous work [13] we have shown that Ni loaded acid Y zeolites exhibited an ethylene productivity of up to  $1.08 \text{ g}_{C_2H_4}/(\text{g}_{\text{cat}} \text{ h})$  with a selectivity of  $\sim 75\%$ . Extended X-ray absorption fine structure (EXAFS) showed that the active Ni catalysts contain both Ni–Ni and Ni–O bonds. In the synthetic method employed in Ref. [13], Ni ions are initially incorporated into the zeolite framework and are subsequently reduced by  $H_2$  to neutral Ni, which then anchors to the inner and/or outer zeolite surface(s).

Zeolite supported transition metal compounds can be prepared in a variety of ways, and the method of preparation can greatly affect the catalytic property of a catalyst as a result of changes in particle size and shape, and oxidation states, etc. For example, Sun and Sachtler [14] have reported three methods of preparation of Mn loaded MFI zeolites (wet-ion-exchange, chemical vapor deposition and solid state ion-exchange), where wet-ion-exchange leads to the highest activity for  $NO_x$  reduction with alkanes.

In this paper we explore a synthetic method for metal ( $M = \text{Fe}, \text{Co}, \text{Ni}, \text{and Cu}$ ) loaded zeolites catalysts for ODHE reactions that differs from what was employed in Ref. [13], and we investigate the catalytic performance of these zeolites and the mechanistic implications of changes in yields as a function of reaction parameters. In the present study, as in Ref [13], the transition metal ions were initially incorporated into the zeolite cationic sites by ion-exchange. They then reacted with the anions in solution ( $OH^-$  and

\* Corresponding author.

E-mail address: [weitz@northwestern.edu](mailto:weitz@northwestern.edu) (E. Weitz).

possibly a small amount of  $\text{PO}_4^{3-}$ ) to form an insoluble salt that, when calcined, is expected to form an oxide that is anchored to the inner and/or outer zeolite surface(s). All catalysts examined in the present work employ a basic zeolitic support with the exchanged ion being  $\text{K}^+$ .

An ethylene selectivity of close to 80% at ethane conversions of >20% was obtained on K–Y supported Ni catalyst. Compared to the Ni/K–Y catalyst, where the Ni component was anchored using  $\text{H}_2$ -treatment [13] (13.7% conversion with 72.9% ethylene selectivity was reported for 100 mg Ni/K–Y) the Ni catalyst reported in this paper gives a higher selectivity for ethylene at a higher  $\text{C}_2\text{H}_6$  conversion. The effects of different reaction conditions are also examined with regard to their mechanistic implications, and information is deduced regarding the relative magnitudes of critical rate constants.

## 2. Experimental

### 2.1. Catalyst preparation

Transition metal ( $\text{M} = \text{Fe}, \text{Co}, \text{Ni}, \text{and Cu}$ ) oxide loaded Y zeolites (Na–Y, Aldrich, with  $\text{Si}/\text{Al} = 2.4$ ) were prepared using ion-exchange in conjunction with subsequent wet impregnation. Ion-exchanges were performed by mixing 200 ml of 0.1 mol/L metal sulfate or nitrate ( $\text{FeSO}_4$ ,  $\text{Co}(\text{NO}_3)_2$ ,  $\text{NiSO}_4$  and  $\text{CuSO}_4$ ) solutions with 6 g Y zeolite (Sodium-form,  $\text{Si}/\text{Al} = 2.4$ , Aldrich). The mixtures were then stirred for 6 h at 88 °C. After filtering, the transition metal-loaded zeolites were washed with large amounts of water and dried at 110 °C. The catalysts obtained are henceforth denoted as M–Y, where  $\text{M} = \text{Fe}, \text{Co}, \text{Ni}, \text{and Cu}$ . The resulting powders were added to 100 ml of 0.8 mol  $\text{K}_3\text{PO}_4$  ( $\text{pH} = 13$ ), and the mixtures were stirred for 2 h at 80 °C. After filtering, the powders were washed with large amounts of water and dried at 110 °C. The resulting catalysts are denoted as M/K–Y type II to distinguish the metal-loaded zeolite catalysts prepared in this study from those prepared in Ref. [13]. For comparison purposes,  $\text{K}^+$  exchanged Y zeolites (K–Y) were prepared by the ion-exchange of 6 g Na–Y with 100 ml 0.8 M  $\text{K}_3\text{PO}_4$  solution at 80 °C that was stirred for 3 h. All as-prepared catalysts were calcined in a He flow at 615 °C for 4 h before catalyst characterization and/or catalytic reaction testing.

### 2.2. Catalyst characterization

The chemical composition of the as-prepared metal-loaded zeolites was determined by inductively coupled plasma atomic emission spectroscopy (ICP-AES, Varian Inc.) using an HF/ $\text{HNO}_3$  solution to dissolve the zeolite samples. X-ray powder diffraction (XRD) patterns were recorded at room temperature on a Rigaku diffractometer ( $\text{Cu-K}\alpha$  radiation, Ni filter, 40 kV, 20 mA,  $2\theta = 10\text{--}70^\circ$ ,  $0.05^\circ$  step size, and 1 s count time). Temperature-programmed reduction experiments with  $\text{H}_2$  ( $\text{H}_2$ -TPR) were performed with a computer controlled flow reactor system (AMI-200, Altamira) equipped with a thermal conductivity detector (TCD). 200 mg of catalyst was placed in a U-tube reactor and exposed to a 30 ml/min flow of 10%  $\text{H}_2$  in Ar while the temperature was increased linearly at a rate of 10 K/min from 50 to 700 °C. The sampling rate of the TCD signal was 1 point every 10 s.

### 2.3. Catalytic reaction tests

The ODH reaction of ethane was typically carried out using 500 mg of catalyst in a tubular quartz micro-reactor operating at atmospheric pressure. The weight of catalyst was varied in order to obtain different  $\text{C}_2\text{H}_6$  conversions at a fixed temperature with a fixed feed flow rate. The reaction feed typically contained

10.3 ml/min  $\text{C}_2\text{H}_6$  (Air gas, purity >99.99%), 10.3 ml/min  $\text{O}_2$  (Air gas, purity >99.98%) and 68.2 ml/min He (Airgas, >99.999%) at 22 °C. The effect of the ratio of  $\text{O}_2$  to  $\text{C}_2\text{H}_6$  in the flow on the yield of and selectivity for  $\text{C}_2\text{H}_4$  was examined by varying the  $\text{O}_2$  flow rate from 5.8 to 10.3 ml/min at a constant ethane and He flow rate. The reaction products were analyzed with a HP 5890 series II gas chromatograph equipped with a TCD. Different columns were used to separate  $\text{CO}_2$ ,  $\text{C}_2\text{H}_4$  and  $\text{C}_2\text{H}_6$  (Porapak Q 80/100) and  $\text{O}_2$  and  $\text{CO}$  (molecular sieve 5A). There was no observable conversion of ethane at 550 °C in either a homogenous gas phase reaction or a reaction over quartz, and there was less than 0.5% conversion of ethane at 600 °C for these reactions. The conversion of  $\text{C}_2\text{H}_6$  ( $X_{\text{C}_2\text{H}_6}$ ) and the selectivity ( $S_{\text{C}_2\text{H}_4}$ ) of  $\text{C}_2\text{H}_4$  and carbon oxides ( $S_{\text{CO}_x}$ ,  $\text{CO}_x = \text{CO}$  or  $\text{CO}_2$ ) are based on the carbon mass balance, which was between 95 and 100%, and was calculated using the following equations:

$$X_{\text{C}_2\text{H}_6} = \frac{[\text{CO}] + [\text{CO}_2] + 2[\text{C}_2\text{H}_4]}{2[\text{C}_2\text{H}_6]_{\text{reactant}}} \times 100\%,$$

$$S_{\text{C}_2\text{H}_4} = \frac{2[\text{C}_2\text{H}_4]}{[\text{CO}] + [\text{CO}_2] + 2[\text{C}_2\text{H}_4]} \times 100\%, \text{ and}$$

$$S_{\text{CO}_x} = \frac{[\text{CO}_x]}{[\text{CO}] + [\text{CO}_2] + 2[\text{C}_2\text{H}_4]} \times 100\%.$$

## 3. Results and discussions

### 3.1. Catalyst characterization

Table 1 lists the chemical compositions of the M–Y and M/K–Y type II zeolites determined from ICP-AES. Based on the M/Al and Na/Al values the transition metal ions replace  $\sim 2/3$  of the exchanged ions in the original Na–Y zeolite. However, the metal loading (i.e. M/Al ratio) does not change (for example, Ni/Al = 0.36 for Ni/K–Y type II and Ni–Y) after treatment using  $\text{K}_3\text{PO}_4$  solutions as evidenced by the fact that  $([\text{K}] + [\text{Na}]) / [\text{Al}]$  is  $\sim 1.0$  for all the M/K–Y type II zeolites. These data show that effectively all the transition metal ions in M–Y zeolites were replaced by the alkali ions after the treatment with  $\text{K}_3\text{PO}_4$  solution. The replaced M ions remained on the zeolitic support as transition metal oxides or hydroxides. Small amounts of P were detected in the M/K–Y type II samples as indicated in the last column of Table 1. The XRD data for the transition metal-loaded Y zeolites, in Fig. 1, show that the as-prepared M/K–Y type II and Ni–Y zeolites exhibit diffraction patterns similar to those for the Na–Y starting material (i.e. they are all missing the metal or oxide phase contribution) [15].

Fig. 2 shows the  $\text{H}_2$ -TPR profiles of the M/K–Y type II and M–Y zeolites. When the Ni and Co loaded zeolites are treated with  $\text{K}_3\text{PO}_4$  solution,  $\text{H}_2$ -reduction occurs at a lower temperature for M/K–Y

**Table 1**

Chemical composition of metal ( $\text{M} = \text{Ni}, \text{Cu}$  and  $\text{Fe}$ ) loaded Y zeolite measured by ICP-AES. The metal to Al ratios are calculated based on the molar concentration, i.e. the  $[\text{M}]/[\text{Al}]$  ratio in the solution for the dissolved samples.

Catalyst	M/Al	Na/Al	K/Al	P/Al
Ni/K–Y type II	0.36	0.06	0.93	0.01
Co/K–Y type II	0.33	0.06	0.95	0.01
Cu/K–Y type II	0.36	0.05	0.95	0.05
Fe/K–Y type II	0.37	0.06	0.05	0.02
Ni–Y	0.36	0.33		
Co–Y	0.34	0.33		
Cu–Y	0.37	0.33		
Fe–Y	0.37	0.30		
Na–Y		0.83		
K–Y		0.06	0.96	

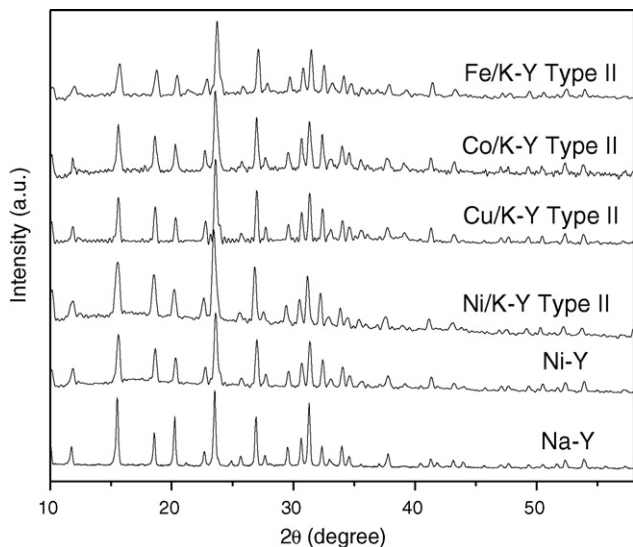


Fig. 1. X-ray diffraction patterns of metal-loaded Y zeolites.

type II relative to the untreated metal-loaded zeolites (M–Y). For instance, for Co–Y, no obvious H<sub>2</sub>-uptake peak was observed in the TPR data (Fig. 2b, dotted line), whereas for Co/K–Y type II, a H<sub>2</sub> reduction peak starts at ~550 °C which extends to higher temperature with a maximum at  $T > 700$  °C. An H<sub>2</sub>-uptake signal was

observed starting at ~350 °C for both Ni–Y and Ni/K–Y type II zeolites. However, above ~425 °C the shape of the H<sub>2</sub>-uptake curve differs markedly for the Ni/K–Y type II and Ni–Y zeolites. For the cases of Cu and Fe, treatment with K<sub>3</sub>PO<sub>4</sub> solution leads to H<sub>2</sub>-reduction taking place at a lower temperature for M/K–Y type II relative to the untreated metal-loaded zeolites (M–Y). A plausible explanation for these differences in reductive behavior relates to the bond energies for the metal–oxygen bonds for the different metals and different synthetic methods. Thus, the structures and/or morphologies of these two sets of zeolites are different.

### 3.2. ODHE reactions on M/K–Y type II catalysts

#### 3.2.1. Effect of the metal

Table 2 presents the catalytic test results for the ODHE reactions at 600 °C. All data in Table 2 were taken using the same O<sub>2</sub> and C<sub>2</sub>H<sub>6</sub> flow rates and are the result of averaging GC data for two runs with a typical difference between runs of less than 2%. Only C<sub>2</sub>H<sub>4</sub>, CO, CO<sub>2</sub>, and a very small amount of CH<sub>4</sub> were observed as reaction products. Because Na–Y and K–Y do not show significant catalytic activity for the ODHE reaction under these conditions, the catalytic conversion observed for the M/K–Y type II catalysts is a consequence of the metal loaded on these supports. From Table 2 it can be seen that the order of activity for these four ODHE catalysts is: Ni > Co > Cu > Fe, which is somewhat different than the order reported for the bulk transition metal oxides (Co > Ni > Fe) [9]. These differences between the unsupported and supported metal oxides could be a result of support effects and/or differences in shape and/or morphology of

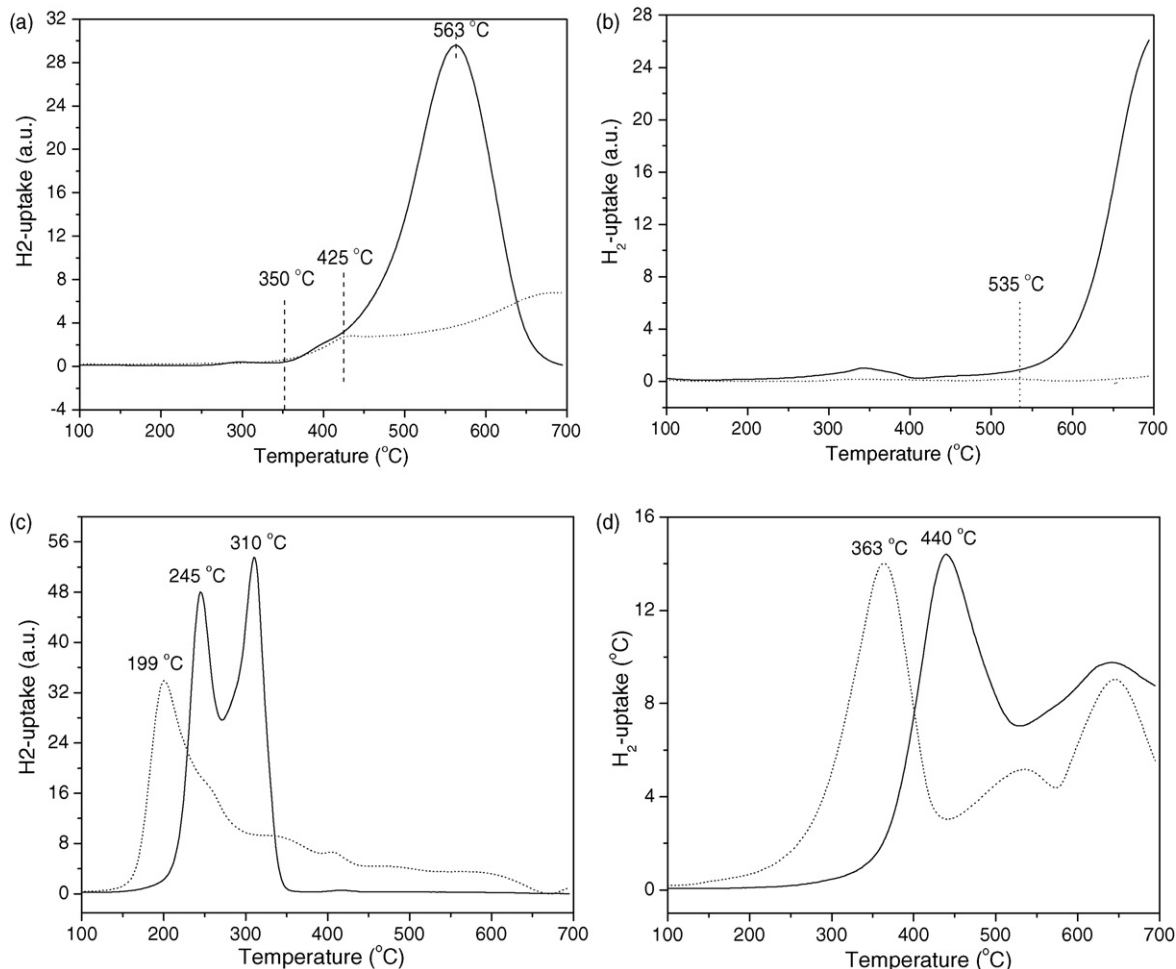


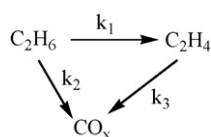
Fig. 2. The H<sub>2</sub>-TPR profiles of 200 mg of M/K–Y type II zeolite (solid lines) and M–Y (dot lines), where M = (a) Ni, (b) Co, (c) Cu and (d) Fe.

**Table 2**

Reaction test result of ODHE on 500 mg M/K–Y type II catalysts listed in the Table.  $T = 600^\circ\text{C}$ . Flow: 10.3 ml  $\text{C}_2\text{H}_6 + 10.3$  ml/min  $\text{O}_2 + 68.2$  ml/min He.

Catalyst	Conversion of $\text{C}_2\text{H}_6$ (%)	Selectivity (%)		
		$S_{\text{C}_2\text{H}_4}$	$S_{\text{CO}}$	$S_{\text{CO}_2}$
Ni/K–Y type II	18.8	77.9	3.4	18.7
Ni–Y	9.4	77.7	11.6	10.7
Ni/KY <sup>a</sup>	13.8	72.9	7.6	19.5
Co/K–Y type II	17.3	30.7	5.0	64.3
Cu/K–Y type II	17.0	23.6	1.8	74.6
Fe/K–Y type II	11.7	35.5	7.8	56.7
Na–Y	0.9	71.0	11.0	18.0
K–Y	1.2	74.6	12.8	12.6

<sup>a</sup> Data were taken from [13]. Weight of catalyst: 100 mg;  $T = 600^\circ\text{C}$ ; Flow: 9.7 ml  $\text{C}_2\text{H}_6 + 3.3$  ml/min  $\text{O}_2 + 62.2$  ml/min He.

**Scheme 1.**

the metal/metal oxide particles. The selectivity for  $\text{C}_2\text{H}_4$  was the highest on Ni/K–Y type II at  $\sim 78\%$ , and the lowest on Cu/K–Y type II at  $\sim 24\%$ .

Ni–Y is less active for ODHE than Ni/K–Y type II (first two rows of Table 2). This may be partly due to  $\text{Ni}^{2+}$  in Ni–Y being harder to reduce than in the Ni/K–Y type II zeolite, which is suggested by the large difference in their  $\text{H}_2$ -TPR profiles (Fig. 2a) in the  $425$ – $700^\circ\text{C}$  temperature range. Compared to the Ni/K–Y catalyst reported previously [13], where the Ni component was anchored as a result of exposure to  $\text{H}_2$ , the Ni/K–Y type II catalysts reported in this paper gives a higher selectivity for ethylene at a higher  $\text{C}_2\text{H}_6$  conversion.

### 3.2.2. Effects of temperature

According to the generally accepted reaction scheme (Scheme 1) for ODHE reactions the initial selectivity (at low conversion of ethane) to  $\text{C}_2\text{H}_4$  depends on the  $k_1/k_2$  ratio, while at higher conversions of ethane, the observed selectivity for production of  $\text{C}_2\text{H}_4$  is associated with the ratio  $k_1/(k_2 + k_3)$  [16,17]. In the following sections the mechanistic implications of our data will be discussed in the context of Scheme 1 above, and Scheme 2, which is discussed in Section 3.3.

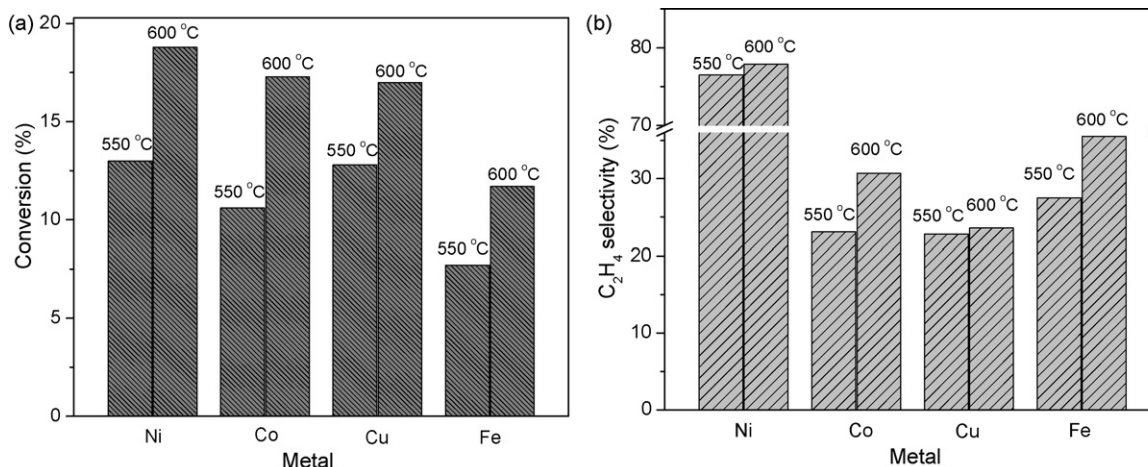


**Fig. 3.** A comparison of the conversion (a) and the selectivity towards  $\text{C}_2\text{H}_4$  (b) for ODHE reactions at  $550$  and  $600^\circ\text{C}$  catalyzed by  $500$  mg M/K–Y type II. Flow:  $10.3$  ml  $\text{C}_2\text{H}_6 + 10.3$  ml/min  $\text{O}_2 + 68.2$  ml/min He.

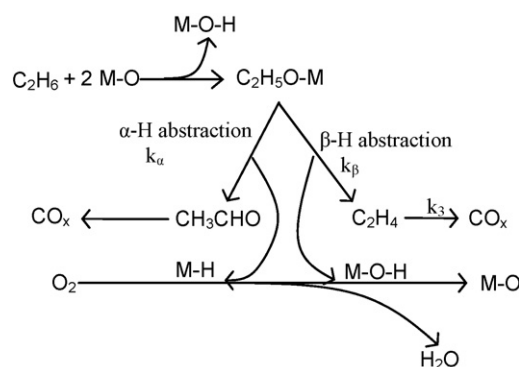
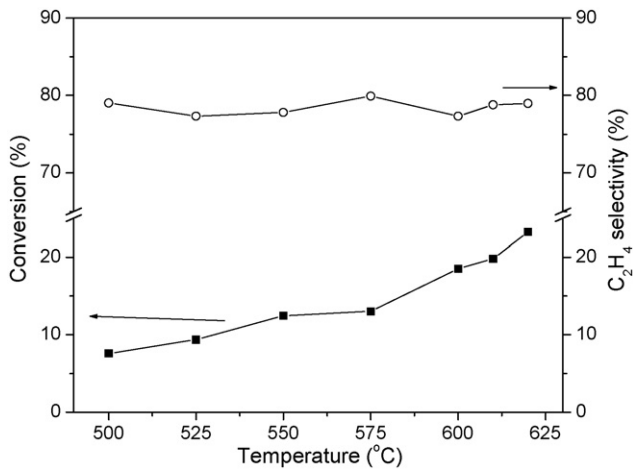
**Scheme 2.** Schematic diagram of a mechanism for catalytic ODHE reactions.

Fig. 3 shows the conversion and selectivity for the ODHE reactions at  $550$  and  $600^\circ\text{C}$  for each metal-loaded zeolite. For all systems, both the conversion of  $\text{C}_2\text{H}_6$  and the observed selectivity for  $\text{C}_2\text{H}_4$  are greater at  $600^\circ\text{C}$  than at  $550^\circ\text{C}$ . That higher temperature favors increased  $\text{C}_2\text{H}_4$  selectivity suggests that these catalysts have similar ODHE reaction mechanisms. Thus for all the M/K–Y type II catalysts examined in this work, the major primary product of oxidation of ethane is  $\text{C}_2\text{H}_4$ , since the selectivity and thus the ratio  $k_1/(k_2 + k_3)$  increases with temperature.

Fig. 4 shows the temperature dependence for  $\text{C}_2\text{H}_6$  conversion and  $\text{C}_2\text{H}_4$  selectivity over  $500$  mg of Ni/K–Y type II catalyst. The  $\text{C}_2\text{H}_4$  selectivity remains at  $\sim 80\%$  as the conversion increases up to over  $23\%$  as the temperature is increased from  $500$  to  $620^\circ\text{C}$  at constant flow rate. The activation energy for a chemical reaction can be obtained by plotting the log of the rate of reaction versus  $1/T$ . However, unless the reaction is elementary this activation energy should be viewed as a phenomenological activation energy that characterizes the temperature dependence of the overall mechanism (or the rate limiting step) for conversion of reactant to product. The data in Fig. 5 allow for the calculation of the phenomenological activation energy for the ODHE reaction on Ni/K–Y type II catalyst of  $51.5 \pm 0.7$  kJ/mol.

### 3.2.3. Effect of the ratio of $\text{O}_2$ and $\text{C}_2\text{H}_6$ flow rates ( $F_{\text{O}_2}/F_{\text{C}_2\text{H}_6}$ ) on conversion and selectivity

For all M/K–Y type II catalysts investigated in this study, the increasing  $F_{\text{O}_2}/F_{\text{C}_2\text{H}_6}$  increases the  $\text{C}_2\text{H}_6$  conversion and lowers the  $\text{C}_2\text{H}_4$  selectivity (see Fig. 6). The decrease in selectivity is relatively small for Ni (9.9%), but significant for Co (33.7%), Cu (25.4%) and



**Fig. 4.** Temperature dependence of the C<sub>2</sub>H<sub>6</sub> conversion and the C<sub>2</sub>H<sub>4</sub> selectivity for ODHE reactions catalyzed by 500 mg Ni/K-Y type II catalyst. The flow was: 10.3 ml C<sub>2</sub>H<sub>6</sub> + 10.3 ml/min O<sub>2</sub> + 68.2 ml/min He.

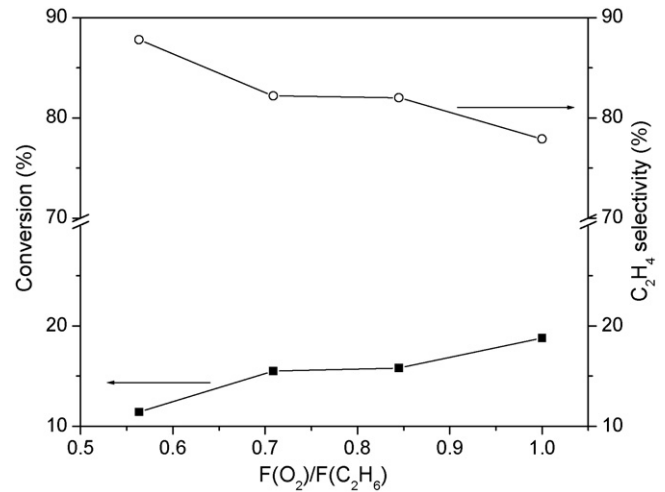


**Fig. 7.** F<sub>O<sub>2</sub></sub>/F<sub>C<sub>2</sub>H<sub>6</sub></sub> dependence of the C<sub>2</sub>H<sub>6</sub> conversion and C<sub>2</sub>H<sub>4</sub> selectivity of the ODHE reaction on 500 mg Ni/K-Y type II at 600 °C.

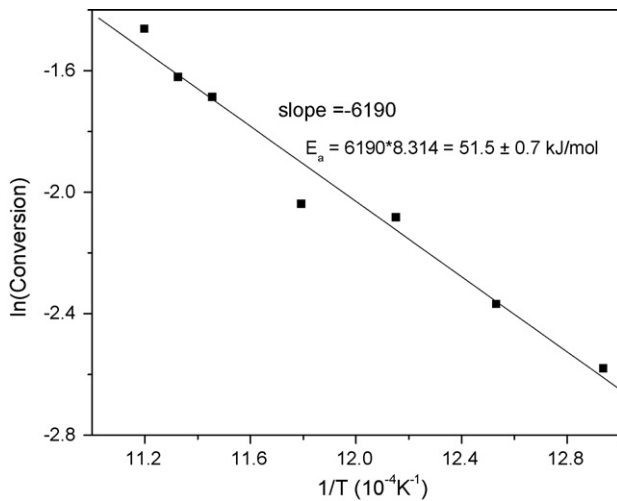


**Fig. 5.** A plot of ln(conversion) of ethane versus 1/T yields the apparent energy of activation for the Ni/K-Y type II catalyzed ODHE reaction. Flow: 10.3 ml C<sub>2</sub>H<sub>6</sub> + 10.3 ml/min O<sub>2</sub> + 68.2 ml/min He.

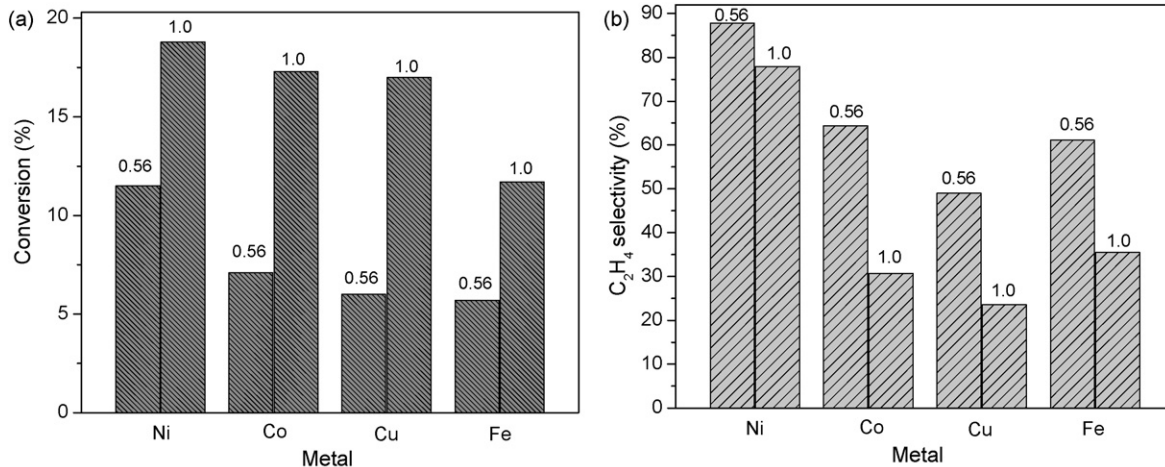


**Fig. 6.** The effect of F<sub>O<sub>2</sub></sub>/F<sub>C<sub>2</sub>H<sub>6</sub></sub> (the number in the figure correspond to the ratio F<sub>O<sub>2</sub></sub>/F<sub>C<sub>2</sub>H<sub>6</sub></sub>) on the C<sub>2</sub>H<sub>6</sub> conversion (left) and C<sub>2</sub>H<sub>4</sub> selectivity for the ODHE reactions. Weight of catalyst: 500 mg. Temperature: 600 °C.

Fe (25.6%). These data suggest that over-oxidation of the desired product (C<sub>2</sub>H<sub>4</sub>) may be relatively more facile for Co, Cu and Fe loaded zeolites than for Ni loaded K-Y zeolites. The  $k_3/k_1$  ratio increases more rapidly as a function of O<sub>2</sub> concentration for Co, Cu and Fe than for Ni. To further characterize the slow decrease in C<sub>2</sub>H<sub>4</sub> selectivity with increasing F<sub>O<sub>2</sub></sub>/F<sub>C<sub>2</sub>H<sub>6</sub></sub> ratio, more data points, were obtained and are shown in Fig. 7. Due to their mitigating effect on the production of carbonaceous deposits, which can lead to catalyst deactivation, O<sub>2</sub> rich flows are desirable during ODH catalysis because they would be expected to enhance catalyst durability. However, an increase in relative concentration of O<sub>2</sub> can lead to more over-oxidation and thus less selectivity for ethylene production.

### 3.3. The C<sub>2</sub>H<sub>4</sub> selectivity at zero conversion (S<sub>0</sub>) for Ni/K-Y type II and their mechanistic implications

From Scheme 1 it can be seen that at very low conversions of ethane the selectivity depends on the ratio  $k_1/k_2$ . Thus, the  $k_1/k_2$  ratio can be estimated from the selectivity in the limit of zero conversion, which we will designate as S<sub>0</sub>, where S<sub>0</sub> is obtained by extrapolating the ethane conversion to zero as discussed in Section 3.2.2.

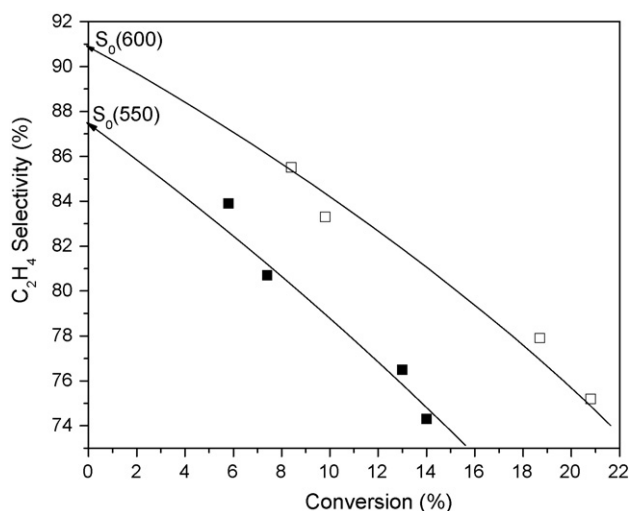


**Fig. 8.** Variation of the C<sub>2</sub>H<sub>4</sub> selectivity as a function of conversion on Ni/K–Y type II at 550 °C (closed rectangles) and 600 °C (open rectangles). Flow: 10.3 ml C<sub>2</sub>H<sub>6</sub> + 10.3 ml/min O<sub>2</sub> + 68.2 ml/min He. S<sub>0</sub>(550) and S<sub>0</sub>(600) are obtained from the extrapolated values for the C<sub>2</sub>H<sub>4</sub> selectivity at zero C<sub>2</sub>H<sub>6</sub> conversion at the respective temperatures.

Kung [18] suggests that the first step for ODH reactions is activation of a C–H bond to form a metal alkyl or metal alkoxide. For the specific case of transition metal oxides, our previous work [13] on the Ni/H–Y catalyzed ODHE reaction allowed us to conclude that the mechanism depicted in Scheme 2, in which the first step of the ODHE reaction is to activate C–H bond in C<sub>2</sub>H<sub>6</sub> to form a metal ethoxide, is consistent with our data. The metal ethoxide could subsequently undergo α-H abstraction to produce an aldehyde or β-H abstraction to produce ethylene. In Scheme 2  $k_{\beta}/k_{\alpha}$  is functionally equivalent to  $k_1/k_2$ , although  $k_1$  is not identical to  $k_{\beta}$  since the rate determining step involves conversion of C<sub>2</sub>H<sub>6</sub> to the ethoxide. Therefore, the C<sub>2</sub>H<sub>4</sub> selectivity at zero conversion ( $S_0$ ) is controlled by  $k_{\beta}/k_{\alpha}$  and this ratio can be estimated from  $S_0$ .

We now focus on the Ni/K–Y type II catalyst.  $S_0$  for Ni/K–Y type II catalyzed ODHE can be estimated by extrapolation of the curve for C<sub>2</sub>H<sub>4</sub> selectivity versus C<sub>2</sub>H<sub>6</sub> conversion (see Figs. 8 and 9). From Fig. 8,  $S_0$  at 550 °C is ~87%, which increase to ~91% at 600 °C. It is not clear the this difference in  $S_0$  is greater than the error limits on  $S_0$ , given that we have a limited number of data points and the curves are generated from a spline fit. However, we have consistently observed an increase in both the yield and selectivity for a given quantity of catalyst when the temperature is increased from 550 to 600 °C. This is compatible with an increase in  $S_0$ . This behavior indicates that in the context of the model in Scheme 2, increased temperature favors β-H abstraction over α-H abstraction [i.e.  $k_{\beta}/k_{\alpha}$  (550) <  $k_{\beta}/k_{\alpha}$  (600)]. Fig. 9 demonstrates that for all O<sub>2</sub>/C<sub>2</sub>H<sub>6</sub> ratios investigated the  $S_0$  values were between ~91 and ~96% (this corresponds to  $k_{\beta}/k_{\alpha}$  in the range of ~10–20). That is, at the temperature of 600 °C, over 90% of C<sub>2</sub>H<sub>6</sub> molecules are converted to C<sub>2</sub>H<sub>4</sub> even in a relatively O<sub>2</sub> rich flow (“O<sub>2</sub> rich” is with respect to the stoichiometric equation for ODHE: C<sub>2</sub>H<sub>6</sub> + 1/2O<sub>2</sub> = C<sub>2</sub>H<sub>4</sub> + H<sub>2</sub>O). We note that the O<sub>2</sub> consumption never reached 100% and though small amounts of CH<sub>4</sub> were observed above 600 °C, hydrogen was not observed, indicating that there was minimal non-oxidative dehydrogenation. Additionally, no acetic acid or acetone was observed in the reaction products. However, a small amount of coke was observed on the catalyst after catalytic testing. As such, a CO<sub>2</sub> peak could be observed when this catalyst was exposed to a flow of O<sub>2</sub> in He. This result indicates that a small amount of non-oxidative dehydrogenation processes does take place above 600 °C.

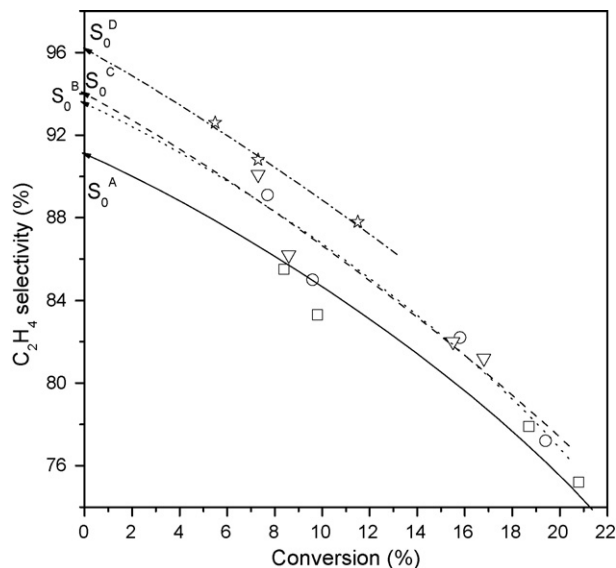


**Fig. 9.** Variation of the C<sub>2</sub>H<sub>4</sub> selectivity for the ODHE reaction as a function of C<sub>2</sub>H<sub>6</sub> conversion on the Ni/K–Y type II catalyst at 600 °C for different O<sub>2</sub>/C<sub>2</sub>H<sub>6</sub> concentration ratios in the reactant flow: (A, rectangles and solid line) 1.0, (B, cycles and dot line) 0.84, (C, triangles and dash line) 0.71 and (D, stars and dash dot line) 0.56. S<sub>0</sub><sup>A</sup>, S<sub>0</sub><sup>B</sup>, S<sub>0</sub><sup>C</sup>, and S<sub>0</sub><sup>D</sup> are the extrapolated values for C<sub>2</sub>H<sub>4</sub> selectivity at a C<sub>2</sub>H<sub>6</sub> conversion of 0%.

The observed change in selectivity and yield of the two sets of catalysts, prepared via different methods (see Section 3.1.1), would typically be rationalized as due to a change in size, composition, and/or morphology of the catalyst particles. However, the fact that the selectivity at low  $S_0$  is associated with the ratio  $k_{\beta}/k_{\alpha}$  indicates that the relative magnitudes of these rate constants change for the different catalysts. Thus, the changes in selectivity cannot be due to simply a surface area resulting from a change in particle size: There must be either a change in particle morphology, most likely leading to preferential exposure of different crystal planes, and/or a change in the steady state proportion of oxide and/or metal.

With the advances in density functional theory (DFT) it has become feasible to attempt to calculate structures and other parameters for reactions on surfaces, including oxide surfaces [19]. Calculations of  $k_a$  and  $k_b$  for metal-loaded zeolites are a potential challenge for such DFT methods. The data obtained in this study could provide a calibration for such calculations, whereas the calculations could provide additional insights into the details of the mechanism for ODHE and why specific metal oxide catalysts exhibit higher yields and selectivities than others.

#### 4. Conclusion

- (1) Four first-row transition metal (Fe, Co, Ni and Cu) oxide loaded K–Y zeolites were synthesized and characterized, and their catalytic performance for ODHE was examined. At 600 °C, for equal concentration of O<sub>2</sub> and C<sub>2</sub>H<sub>6</sub>, the ODHE activity follows the order: Ni > Co > Cu > Fe and the C<sub>2</sub>H<sub>4</sub> selectivity is: Ni > Co ≈ Fe > Cu. The Ni/K–Y type II catalyst can give a higher selectivity for ethylene at higher C<sub>2</sub>H<sub>6</sub> conversions than previously reported for a Ni/K–Y catalyst prepared via a different method.
- (2) Increasing reaction temperature leads to a modest increase in selectivity for all M/K–Y type II systems. The apparent energy of activation for the reaction of ethane on Ni/K–Y type II is  $51.5 \pm 0.7$  kJ/mol.
- (3) Increasing the concentration of O<sub>2</sub> (F<sub>O<sub>2</sub></sub>) relative to C<sub>2</sub>H<sub>6</sub> (F<sub>C<sub>2</sub>H<sub>6</sub></sub>) in the reactant flow leads to an increase in the conversion of

- $C_2H_6$ , but a decrease in the  $C_2H_4$  selectivity. The influence of  $F_{O_2}/F_{C_2H_6}$  on the  $C_2H_4$  selectivity is relatively small for Ni/K–Y type II, but more significant for the other M/K–Y type II zeolites.
- (4) The  $C_2H_4$  selectivity at zero conversion ( $S_0$ ) on Ni/K–Y type II was obtained by extrapolation of the yield to zero. The values for  $S_0$  are consistent with the rate of  $\beta$ -H abstraction being at least 10 times that of the rate of  $\alpha$ -H abstraction from a metal ethoxide formed from ethane via an ethyl radical intermediate.

#### Acknowledgments

This work was supported by the Chemical Sciences, Geosciences and Biosciences Division, Office of Basic Energy Sciences, Office of Science, U.S. Department of Energy (DE-FG02-03-ER15457), at the Northwestern University Institute for Catalysis in Energy Processes. This work made use of the J.B. Cohen X-ray Facility supported by the MRSEC program of the National Science Foundation (DMR-0520513) at the Materials Research Center of Northwestern University.

#### References

- [1] Chemical & Engineering News 84 (2006) 59.
- [2] K. Weissmehl, H.-J. Arpe, *Industrial Organic Chemistry* (C.R. Lindley, Trans.) 3rd completely rev. ed., VCH, Weinheim, 1997, p. 59 (Chapter 3).
- [3] F. Cavani, N. Ballarini, A. Cericola, *Catal. Today* 127 (2007) 113.
- [4] F. Cavani, F. Trifirò, *Catal. Today* 51 (1999) 561.
- [5] L. Čapek, J. Adam, T. Grygar, R. Bulánek, L. Vradman, G. Košová-Kučerová, P. Čičmanec, P. Knotek, *Appl. Catal. A* 342 (2008) 99.
- [6] T. Blasco, A. Galli, J.M. Lopez Nieto, F. Trifirò, *J. Catal.* 169 (1997) 203.
- [7] G. Tsilomelekis, A. Christodoulakis, S. Boghosian, *Catal. Today* 127 (2007) 139.
- [8] C. Liu, U.S. Ozkan, *J. Mol. Catal.* 220 (2004) 53.
- [9] Y. Schuurman, V. Ducarme, T. Chen, W. Li, C. Mirodatos, G.A. Martin, *Appl. Catal. A* 163 (1997) 227.
- [10] X. Zhang, J. Liu, Y. Jing, Y. Xie, *Appl. Catal. A* 240 (2003) 143.
- [11] K.-I. Nakamura, T. Miyake, T. Konishi, T. Suzuki, *J. Mol. Catal. A* 260 (2006) 144.
- [12] P. Concepcion, T. Blasco, J.M. Lopez Nieto, A. Vidal-Moya, A. Martinez-Arias, *Micropor. Mesopor. Mater.* 67 (2004) 215.
- [13] X.-F. Lin, C.A. Hoel, W.M.H. Sachtler, K.R. Poeppelmeier, E. Weitz, *J. Catal.* 265 (2009) 54.
- [14] Q. Sun, W.M.H. Sachtler, *Appl. Catal. B* 42 (2003) 393.
- [15] B.-Z. Zhan, E. Iglesia, *Angew. Chem. Int. Ed.* 46 (2007) 3697.
- [16] J.M. Blasco, López Nieto, *Appl. Catal. A* 157 (1997) 117.
- [17] M.D. Argyle, K. Chen, A.T. Bell, E. Iglesia, *J. Phys. Chem. B* 106 (2002) 5421.
- [18] H.H. Kung, *Adv. Catal.* 40 (1994) 1.
- [19] M.S. Palmer, M. Neurock, M.M. Olken, *J. Am. Chem. Soc.* 124 (2002) 8452.